Project "Evaluation and Diagnosis of the Atlantic Meridional Overturning Circulation 3D Structure in Climate Models" (Grant # NA15OAR4310088)-**Final Report**

PIs: Xiaobiao Xu (COAPS/FSU), Eric P. Chassignet (COAPS/FSU), Molly O. Baringer (AOML/NOAA), and Shenfu Dong (AOML/NOAA)

Main goals of the Project

The overall goals of this project are 1) to derive a better and more comprehensive diagnosis for evaluating the Atlantic meridional overturning circulation (AMOC) representation, including time mean structure and temporal variability, in the Coupled Model Inter-comparison Project (CMIP5) models, and 2) to identify and understand the key physical processes or mechanisms that lead to the wide spread of the AMOC state among the CMIP5 as well as the AMOC variability in individual models.

Results and Accomplishments

During this project, we conducted several researches related to the temperature and salinity structure and the associated (diapycnal) water mass transformation of the AMOC in both high-resolution ocean simulations and low-resolution fully coupled climate models. On the observations (AMOL/NOAA), we quantified the AMOC variability at 34.5°S using different observation techniques, including XBT, Argo data in combinations with WOA-13 climatology, and six years of moored observations near the western and eastern boundaries of the South Atlantic, in combination with satellite winds. The key results include

1. On the temperature and salinity structure of the North Atlantic circulation. We found that the North Atlantic circulation can be separated into the large-scale Atlantic meridional overturning circulation (AMOC) that is diapycnal and the subtropical and subpolar gyres that largely flow along isopycnal surfaces but also include prominent gyre-scale diapycnal overturning in the Subtropical Mode Water and Labrador Sea Water, respectively. One natural way of depicting meridional heat/freshwater exchange through the ocean circulation is to project the trans-basin meridional transport on potential temperature θ and salinity S (θ-S) plane, which includes not only the dispycnal transformation, but also the effects of isopycnic mixing and the related water mass transformation through "spice" change (see Figure 1 for an example of the transport on (θ-S) plane across 4 important latitudes in the Atlantic Ocean). Integrals of the meridional volume transport as a function of θ and S yield streamfunctions with respect to θ and to S, and heat functions. These argue for a significant contribution to the heat transport by the southward circulation of North Atlantic Deep Water. In the subtropics at 26.5°N, the isopycnic component of the subtropical gyre is colder and fresher in the northward-flowing western boundary currents than the southward return flows, and it carries heat southward and freshwater northward, opposite of that of the diapycnal component. When combined, the subtropical gyre contributes virtually zero to the heat transport and the AMOC is responsible for all the heat transport across this latitude. The subtropical gyre however significantly contributes to the freshwater transport, reducing the 0.5 Sv southward AMOC freshwater transport by 0.13 Sv. These results clarified the different roles of the basin-scale AMOC and the sub-basin scale (lateral) gyres in transporting heat and freshwater meridionally.

2. On the structure of the diapycnal transformation associated with the upper limb of the Atlantic meridional overturning circulation (AMOC). Diapycnal water mass transformation is the essence behind the AMOC and the associated heat/freshwater transports. Existing studies have mostly focused on the transformation that is directly forced by surface buoyancy fluxes, and the role of interior mixing is much less known. We mapped the three-dimensional structure of the diapycnal transformation, both surface-forced and mixing induced, using results of a high-resolution numerical model that have been shown to represent the large-scale structure of the AMOC and the North Atlantic subpolar/subtropical gyres well. The analyses show that 1) annual mean transformation takes place seamlessly from the subtropical to the subpolar North Atlantic following the surface buoyancy loss along the northward-flowing upper AMOC limb (Figures 2-3 in subtropical and subpolar regimes); 2) mixing, including wintertime convection and warm-season restratification by mesoscale eddies in the mixed layer and submixed layer diapycnal mixing, drives transformations of Subtropical Mode Water in the southern part of the subtropical gyre and Labrador Sea Water in the Labrador Sea and on its southward path in the western Newfoundland Basin; and 3) patterns of diapycnal transformations toward lighter and denser water do not align zonally. Thus, the net three-dimensional transformation is significantly stronger than the zonally integrated, two-dimensional AMOC streamfunction (50% in the southern subtropical North Atlantic and 60% in the western subpolar North Atlantic).

3. On the AMOC variability between the atmospherically-forced ocean models and fully-coupled climate models. We examined the basic characteristics of the AMOC variability in 44 CMIP5 (Phase 5 of the Coupled Model Inter-comparison Project) simulations, using the 18 atmospherically-forced CORE-II (Phase 2 of the Coordinated Ocean-ice Reference Experiment) simulations as a reference (Figure 4). The analysis shows that on interannual and decadal timescales, the AMOC variability in the CMIP5 exhibits a similar magnitude and meridional coherence as in the CORE-II simulations, indicating that the modeled atmospheric variability responsible for AMOC variability in the CMIP5 is in reasonable agreement with the CORE-II forcing. On multi-decadal timescales, however, the AMOC variability is weaker by a factor of more than 2 and meridionally less coherent in the CMIP5 than in the CORE-II simulations. The CMIP5 simulations also exhibit a weaker long-term atmospheric variability in the North Atlantic Oscillation (NAO). However, one cannot fully attribute the weaker AMOC variability to the weaker variability in NAO because, unlike the forced CORE-II simulations, the coupled CMIP5 simulations do not exhibit a robust NAO-AMOC linkage (Figure 5). The reason is that while the variability of the wintertime heat flux and mixed layer depth in the western subpolar North Atlantic is strongly linked to the AMOC variability, the NAO variability is not.

4. On the water mass properties of the AMOC components and the relationship to the heat and freshwater transports in the CMIP5 models. Similar to high-resolution study, we examined the temperature-salinity (θ-S) characteristic of the AMOC in climate models and found that, while the magnitude of the oceanic heat transport is closely correlated with the magnitude of the AMOC transports, not the temperature bias. The temperature bias plays a fundamental role in systematically lower than heat transport presented in 20-CMIP5 models. The salinity of the upper and lower limbs of the AMOC plays an even larger role in the oceanic salinity (or freshwater) transports: the magnitude of the salinity transport in different CMIP5 models is directly correlated with the salinity difference between the upper and lower

limbs of the AMOC, not the magnitude of the AMOC transports (Figure 6). This highlights the importance of representing temperature salinity water properties in CMIP5 models.

5. The Iceland-Scotland overflow water (ISOW) is an important component of the North Atlantic deep water in the lower limb of the Atlantic meridional overturning circulation. This water mass flows southward along western side of the Iceland Basin and exits the basin through multiple pathways. One of the most important and substantially observed pathway is through the Charlie Gibbs Fracture Zone, where moored observations show large fluctuations of the ISOW transport (Figure 7). We found that the 1/12° eddying HYCOM simulation reproduced most of the observed ISOW transport variability through the CGFZ. The analysis show that a) the variability of the ISOW transport is closely correlated with that of the barotropic transports in the CGFZ associated with the meridional displacement of the North Atlantic Current front and is possibly induced by fluctuations of large-scale zonal wind stress in the Western European Basin east of the CGFZ; b) the variability of the ISOW transport is increased by a factor of 3 from the northern part of the Iceland Basin to the CGFZ region and transport time series at these two locations are not correlated, further suggesting that the variability at the CGFZ does not come from the upstream source; and c) the variability of the ISOW transport at the CGFZ is strongly anticorrelated to that of the southward ISOW transport along the eastern flank of the Mid-Atlantic Ridge, suggesting an out-of-phase covarying transport between these two ISOW pathways.

6. We Studied the AMOC-associated circulation in the South Atlantic Ocean and the latitudinal coherence of the AMOC, using model outputs from a 60-year, 1/12° global ocean-sea ice simulation that is forced with the latest atmospheric forcing JRA-55. The modeled results are validated against observations at a zonal section at 34°S, a meridional section at 65°W in the Drake Passage, and a meridional section southwest of Africa. We find that, first, the upper limb of the AMOC originates from the Agulhas leakage. The direct contribution of cold Pacific water from the Drake Passage to the AMOC is small, the cold water does flow into the subtropical gyre of the South Atlantic and modify the temperature and salinity properties of the water there (Figure 8), therefore it impacts the meridional heat/freshwater transports. Second, the North Atlantic deep water (NADW) in the lower limb of AMOC flows southward as a deep western boundary current all the way to 45°S and then turns eastward to flow across the Mid-Atlantic Ridge near 42°S. The recirculation around the Vitoria Trindade seamount chain brings some NADW into the Brazil Basin interior. A revised manuscript is to be submitted to the *JGR-Ocean.*

7. Two years of observations from the French/South African CPIES array near the eastern boundary along 34.5°S were analyzed to evaluate the mean structure of the eastern boundary currents (EBC), the associated water masses, and the volume transport variability. The estimated northward time-mean Benguela Current transport is 24 Sv, with a temporal standard deviation of 17 Sv. Beneath this current the time-mean transport is southward, indicating the presence of a deep-EBC (DEBC), with a time-mean transport of 12 Sv, and a standard deviation of 17 Sv. Offshore of these currents, the shallow and deep flows are more variable with weak time means, likely influenced by Agulhas Rings transiting through the region. Hydrographic data collected along the CPIES line demonstrate that the DEBC is carrying recently ventilated North Atlantic Deep Water, as it flows along the continental slope. This is consistent with a previously hypothesized interior pathway bringing recently

ventilated North Atlantic Deep Water from the Deep Western Boundary Current across the Atlantic to the Cape Basin. The observations further indicate that much of the DEBC must recirculate within the basin.

Highlights of Accomplishments

1. We examined the temperature-salinity structure of North Atlantic circulation and their role in the meridional heat/fresh water transports; then mapped spatial distributions and physical mechanisms (surface-buoyancy forcing versus horizontal mixing in the surface mixed layer) of the diapycnal water mass transformation associated with the upper limb of AMOC.

2. We studied the variability of the AMOC in the coupled CMIP5 model in comparison to the atmospherically-forced COREII simulations of similar resolution, and quantified the water mass properties of the AMOC represented in the CMIP5 models and their impacts to the modeled heat and freshwater transports.

3. We quantified the AMOC variability at 34.5°S using six years of moored observations near the western and eastern boundaries of the South Atlantic, in combination with satellite winds.

4. We completed a 60-year integration of the global ocean-sea ice simulation based on HYCOM and CICE, using the latest atmospheric forcing product JRA55 and, along with the observations obtained at 34.5°S and other places, we studied the circulation pathways of the upper and lower limbs of the AMOC in the South Atlantic.

Transitions to Applications

The AMOC temperature-salinity structure diagnose tools are included as part of the NOAA-MAPP MDTF process-oriented diagnostic package.

Estimate of current technical readiness level of work

Most of the research work performed in this project are of RL 1: Basic Research, i.e., to improve our understanding of the water properties, and water mass transformation of the Atlantic Circulation. Part of the research works, i.e., the AMOC temperature-salinity structure diagnose tools, is of RL 2: Applied research, and can be used to diagnose the AMOC structure in climate models.

Publications from the Project

Baringer, M. O., J. Willis, D. A. Smeed, B. Moat, S. Dong, W. R. Hobbs, D. Rayner, W. E. Johns, G. Goni, M. Lankhorst, and U. Send, Global oceans—Meridional overturning and oceanic heat transport circulation observations in the North Atlantic Ocean, In *State of the Climate in 2017*, J. Blunden, D.S. Arndt, and G. Hartfield (eds.), *Bulletin of the American Meteorological Society*, 99 (8), S91-S94, doi: 10.1175/2018BAMSStateoftheClimate.1, 2018.

Frajka-Williams, E., Ansorge, I.J., Baehr, J., Bryden, H.L., Chidichimo, M.P., Cunningham, S.A., Danabasoglu, G., Dong, S., Donohue, K.A., Elipot, S., Heimbach, P., Holliday, N.P., Hummels, R., Jackson, L.C., Karstensen, J., Lankhorst, M., Le Bras, I., Lozier, M.S., McDonagh, E.L., Meinen, C.S., Mercier, H., Moat, B.I., Perez, R.C., Piecuch, C.G., Rhein, M., Srokosz, M.A., Trenberth, K.E., Bacon, S., Forget, G., Goni, G., Kieke, D., Koelling, J., Lamont, T., McCarthy, G.D., Mertens, C., Send, U., Smeed, D.A., Speich, S., van den Berg, M., Volkov, D., and Wilson, C., 2019: Atlantic Meridional Overturning Circulation: Observed transport and variability. Frontiers in Marine Science, 6:260 (doi:10.3389/fmars.2019.00260).

Kersale, M., R.C. Perez, S. Speich, C.S. Meinen, T. Lamont, M. Le Henaff, M.A. van den Berg, S. Majumder, I.J. Ansorge, S. Dong, C. Schmid, T. Terre, and S. L. Garzoli, 2019, Shallow and deep eastern boundary currents in the South Atlantic at 34.5S: Mean structure and variability. *Journal of Geophysical Research: Oceans*, 124, 1634-1659.

Lee, S.-K., R. Lumpkin, M.O. Baringer, C.S. Meinen, M. Goes, S. Dong, H. Lopez, and S.G. Yeager, 2019: Global meridional overturning circulation inferred from a data-constrained ocean and sea-ice model. *Geophysical Research Letters*, 46(3):1521-1530, doi:10.1029/2018GL080940.

Lopez, H., G. Goni, and S. Dong. A reconstructed South Atlantic Meridional Overturning Circulation time series since 1870. Geophysical Research Letters, 44(7):3309-3318, doi:10.1002/2017GL073227 2017

Maloney, E., A. Gettelman, Y. Ming, J. D. Neelin, D. Barrie, A. Mariotti, C.-C. Chen, D. R. B. Coleman, Y.-H. Kuo, B. Singh, H. Annamalai, A. Berg, J. F. Booth, S. J. Camargo, A. Dai, A. Gonzalez, J. Hafner, X. Jiang, X. Jing, D. Kim, A. Kumar, Y. Moon, C. M. Naud, A. H. Sobel, K. Suzuki, F. Wang, J. Wang, A. Wing, X. Xu, and M. Zhao, 2019, Process-oriented evaluation of climate and weather forecasting models, *Bulletin of the American Meteorological Society doi:10.1175/BAMS-D-18-0042.1*

Meinen, C.S., Speich, S., Piola, A.R., Ansorge, I., Campos, E., Kersalé, M., Terre, T., Chidichimo, M.P., Lamont, T., Sato, O.T., Perez, R.C., Valla, D., Van den Berg, M., Le Hénaff, M., Dong, S., and Garzoli, S.L., 2018: Meridional Overturning Circulation transport variability at 34.5°S during 2009-2017: Baroclinic and barotropic flows and the dueling influence of the boundaries. Geophysical Research Letters, 45(9):4180-4188 doi:10.1029/2018GL077408.

Xu, X., P. B. Rhines, and E. P. Chassignet, 2016, Temperature-salinity structure of the North Atlantic circulation and associated heat and freshwater transports, *J. Climate.* **29**(21), 7723-7742, doi:10.1175/JCLI-D-15-0798.1.

Xu, X., P. B. Rhines and E. P. Chassignet, 2018, On mapping the diapycnal water mass transformation of the upper North Atlantic Ocean, *Journal of Physical Oceanography*, doi:10.1175/JPO-D-17-0223.1

Xu, X., A. Bower, H. Furey, and E. P. Chassignet, 2018, Variability of the Iceland-Scotland overflow water transport through the Charlie-Gibbs Fracture Zone: Results from an eddying simulation and observations, Journal of Geophysical Research: Oceans, 123, 5808–5823, doi:10.1029/2018JC013895

Xu, X., E. P. Chassignet and F. Wang, 2019, On the variability of the Atlantic meridional overturning circulation transports in coupled CMIP5 simulations, *Climate Dynamics. doi:10.1007/s00382-018-4529-0*

Xu, X., E. P. Chassignet, S. Dong, and M. Baringer, 2019, Transport structure of the South Atlantic Ocean derived from a high-resolution numerical model and observations, a manuscript to be resubmitted to *Journal of Geophysical Research: Oceans*

PI Contact information

Xiaobiao Xu (xxu3@fsu.edu)

Center for Ocean-Atmospheric Prediction Studies (COAPS)/FSU
2000 Levy Avenue, Building A, Room 263
Tallahassee, FL 32310
850-644-6931 (Tel)
850-644-4841 (Fax)
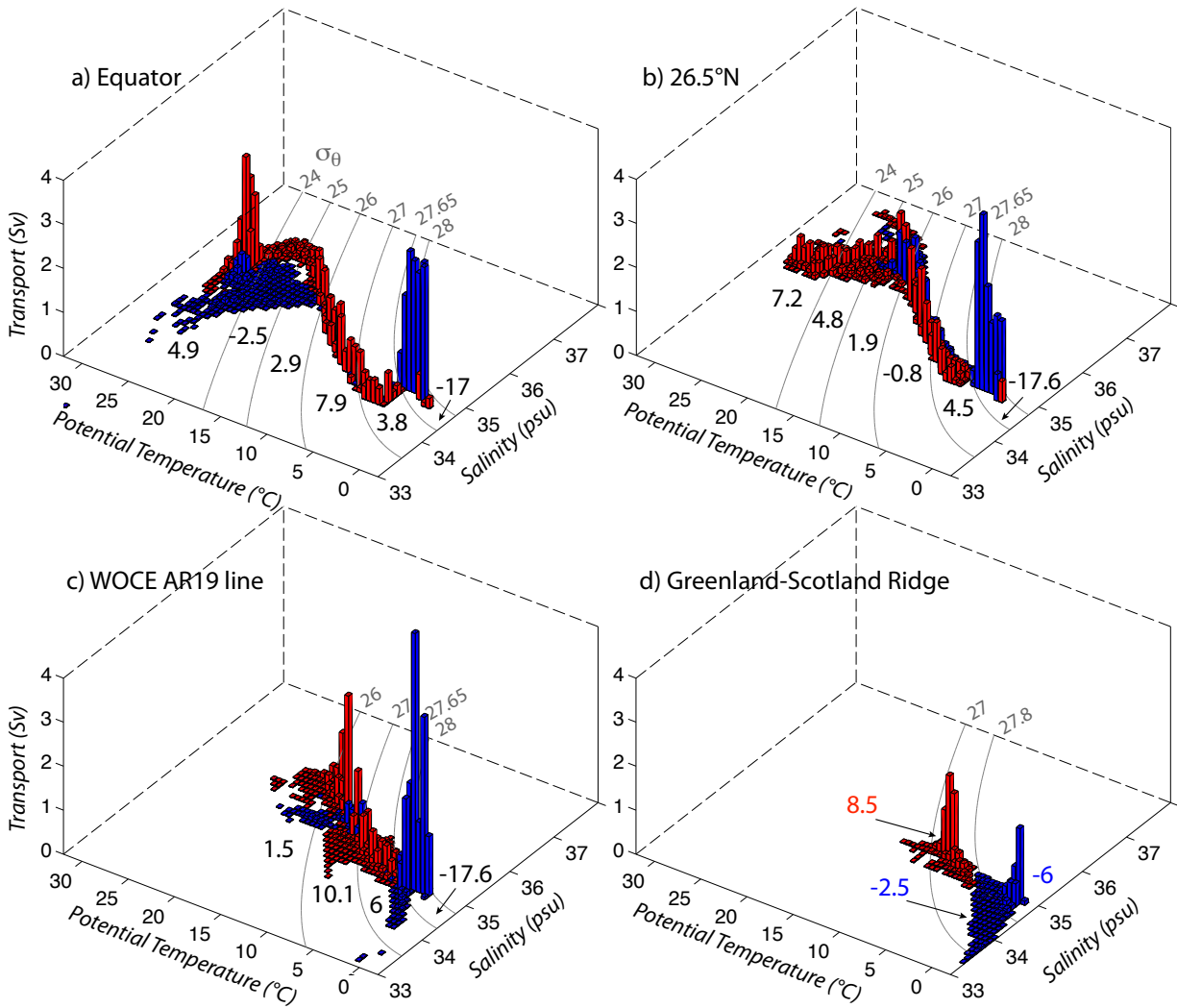
Figure 1. Modeled mean meridional transport projected onto the temperature-salinity (θ-S) plane across four trans-Atlantic sections: a) Equator, 2) RAPID line at 26°N, WOCE AR19 line near 48°N, and Greenland-Scotland Ridge. Red (blue) bars denote north-/south-ward transports within a $\Delta\theta \times \Delta S$ box of 0.5°C×0.1psu. The black numbers are the net transports for each density layers; The red/blue numbs are north-/south-ward transports for the three water masses defined in Eldevik and Nilsen (2013).
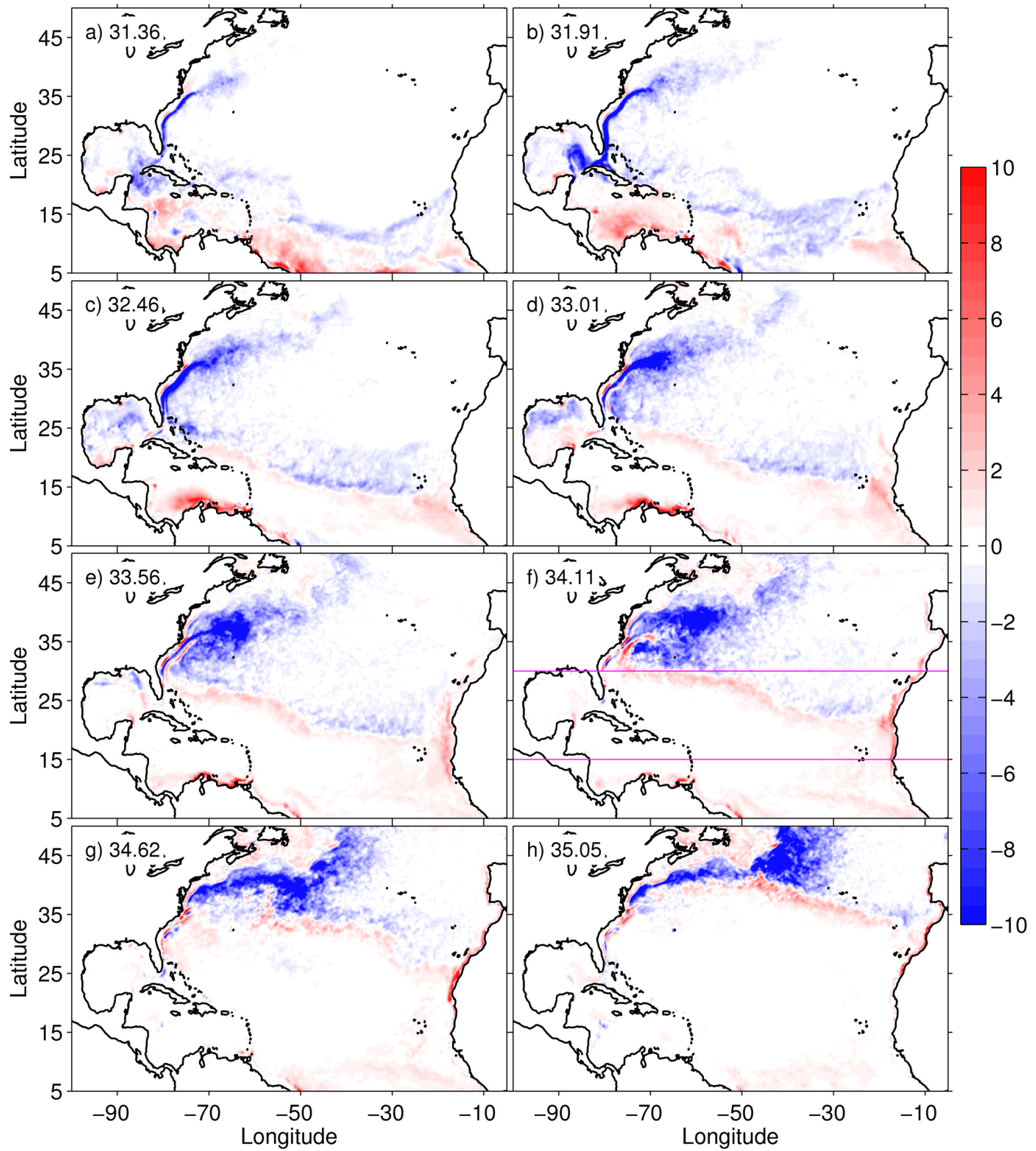
Figure 2. Distribution of modeled time mean total diapycnal transformation per unit area (in velocity unit of 10^{-6} m s^{-1}) across a series of 8 density surfaces in the subtropical North Atlantic. The blue color shading illustrates a progress light-to-dense transformation from the Florida Current-Gulf Stream-North Atlantic Current. The red color shows dense-to-light transformation that takes place in the subtropical gyre.
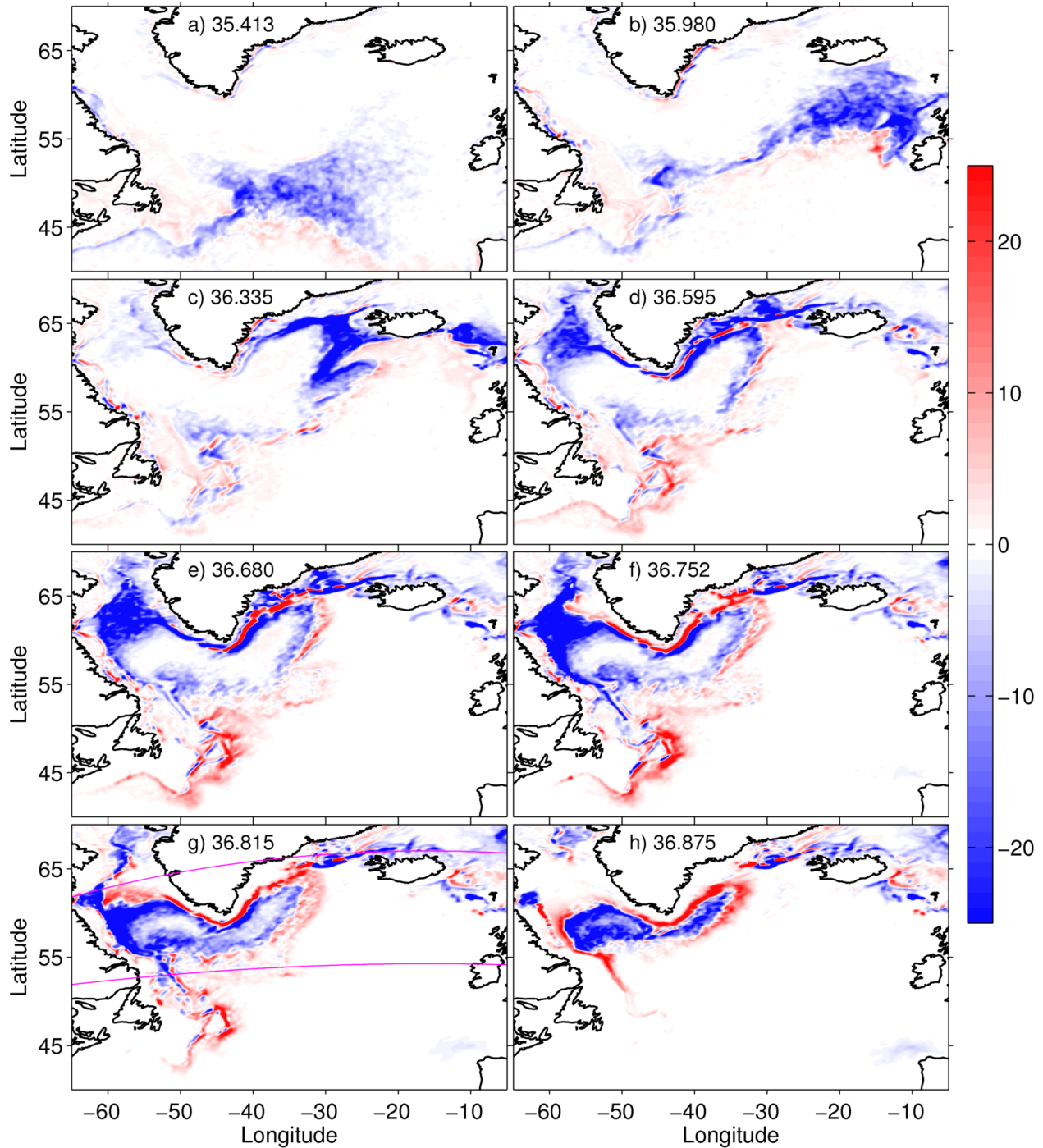
Figure 3. Distribution of the modeled time-mean, total diapycnal transformation per unit area (in velocity unit of 10^{-6}m s^{-1}) across a series of 8 density surfaces in the subpolar North Atlantic. Together with Figure 2, the blue color shading illustrates a seamless light-to-dense transformation from the subtropical to subpolar regimes (through the North Atlantic Current). The red color shows the mixing induced dense-to-light transformation that takes place around the subpolar gyre.
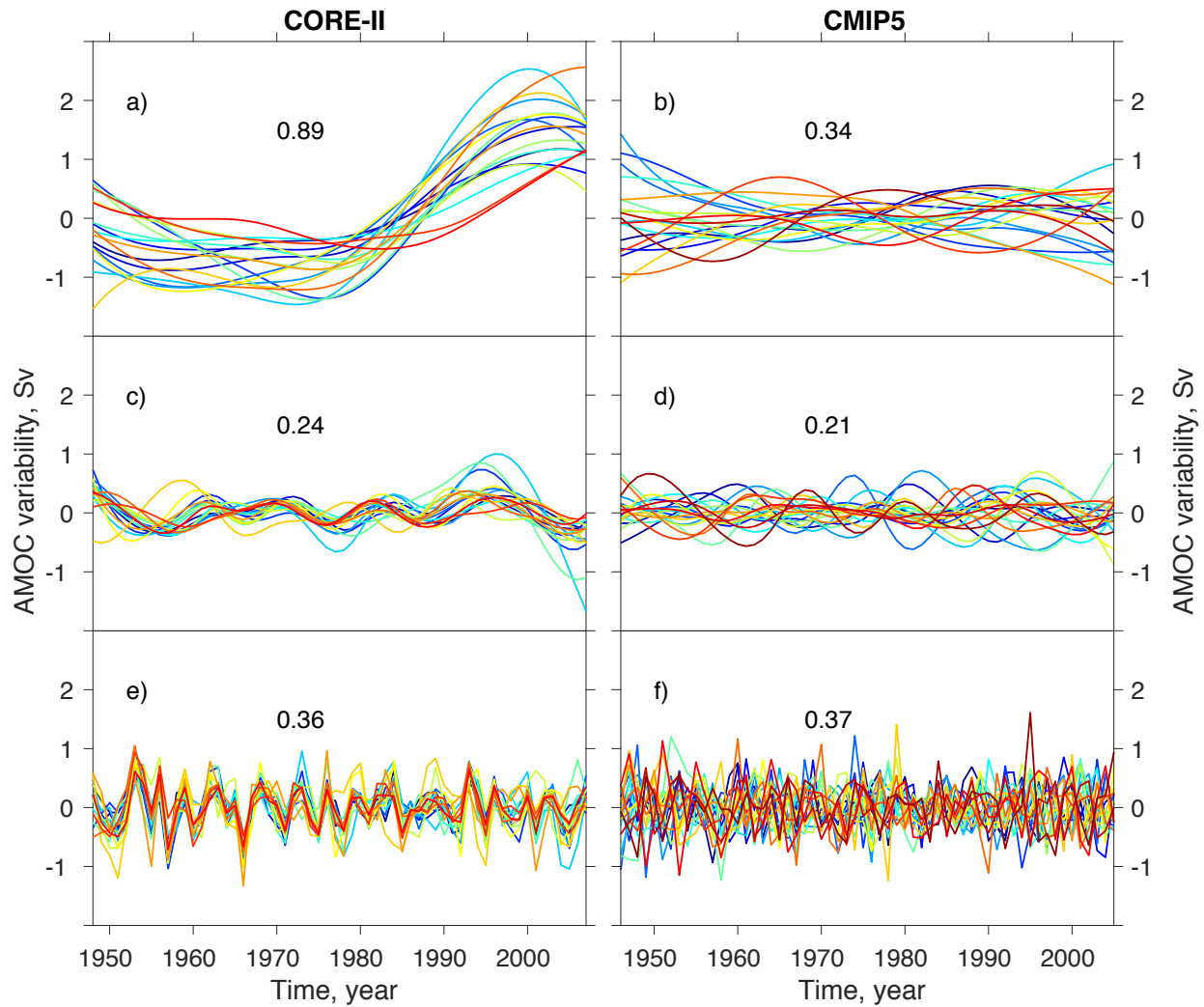
Figure 4. Variability of the basin-wide averaged AMOC transports (in Sv) from 30°S to 60°N in the 18 atmospherically-forced COREII simulations and 44 fully-coupled CMIP5 simulations at different timescales: a-b, multidecadal; c-d) decadal; and e-f interannual. The colored lines represent individual simulations and the numbers are multi-model averages of the standard deviation for each timescale. The results illustrate that the multidecadal variability is much higher (and more consistent) in CORE-II than in the CMIP5 simulations. The magnitude of the decadal and interannual variabilities is comparable between the CORE-II and CMIP5 simulations.
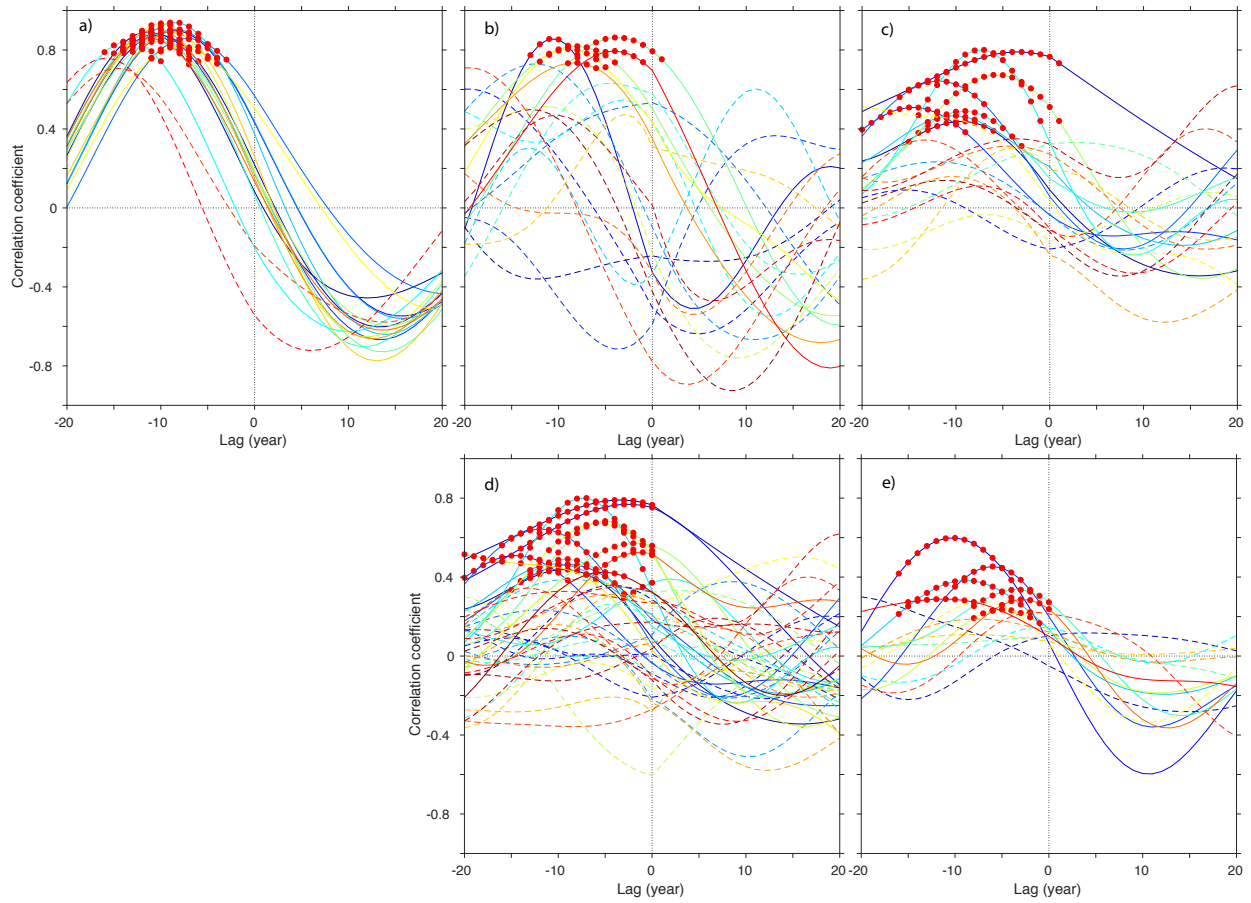
Figure 5. Lead-lag correlation between the station-based wintertime NAO index and the basin-wide averaged AMOC variability in a) 18 CORE-II simulations from 1948-2007; b) 20 historical CMIP5 simulation that has the same ocean component as in CORE-II simulations for 1946-2005; c) same 20 historical CMIP5 simulation for full 150 years (1850-2005); d) 44 CMIP5 simulation for full integration period; and e) 15 pi-control simulation for their record length ranging from 250 to 1000 years. The Negative lag values indicate that the NAO leads the AMOC. Color lines represent individual simulation. Solid lines indicate significant NAO-AMOC correlation (at 90% levels) whereas the dashed lines denote the correlation is weak (insignificant). The results highlighted a fundamental difference, that is the NAO-AMOC is significant/robust in forced CORE-II simulations, but not in fully-coupled CMIP5 simulations.
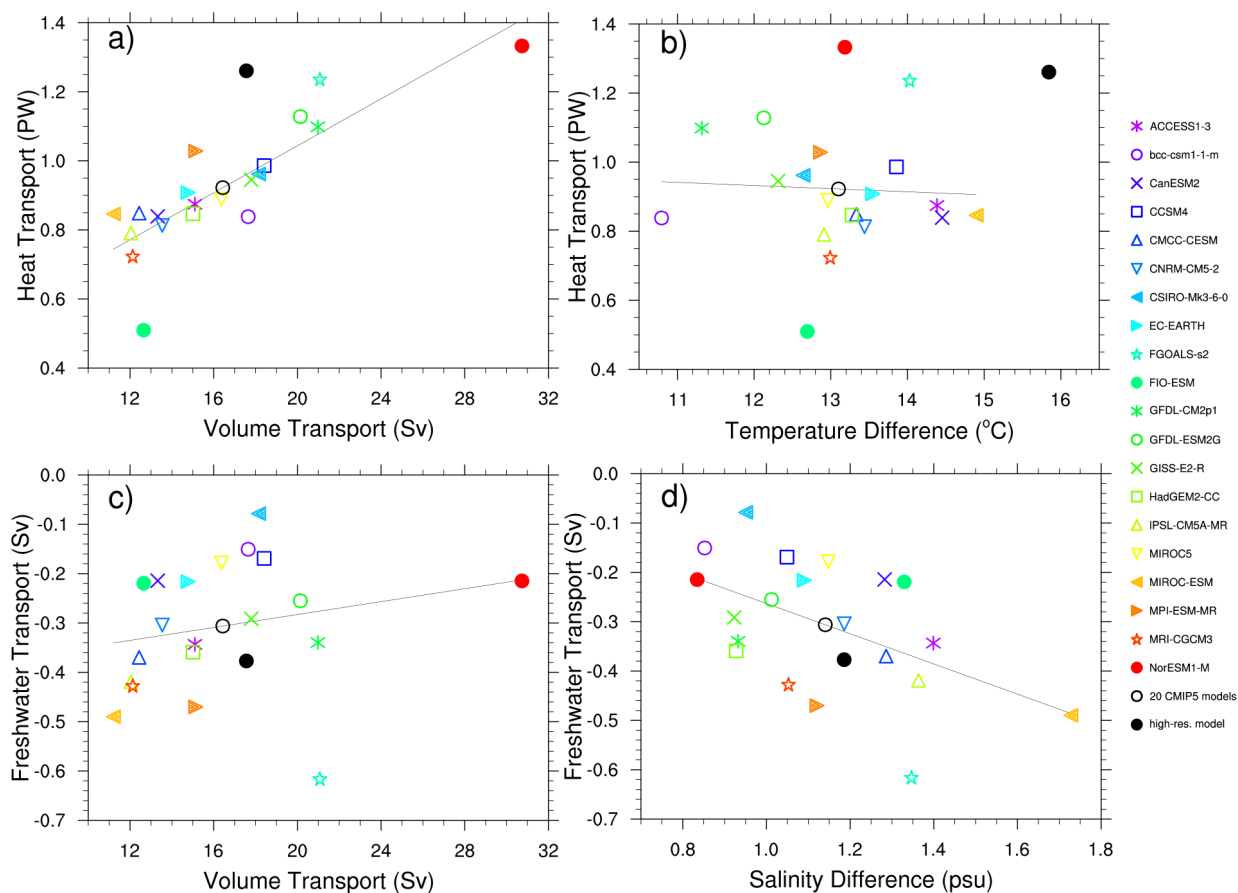
Figure 6. Relation of the modeled oceanic heat transport with (a) volume transport and (b) temperature difference (between the upper and lower AMOC limbs) at 26°N. Relation of the modeled freshwater transport with (c) volume transport and (d) salinity differences. Colored symbols and the black circle denote results from 20 CMIP5 historical simulations and their average, respectively; black dot denotes high-resolution ocean simulation results that represent well the observed mean heat and freshwater transports and the AMOC structure at 26°N.
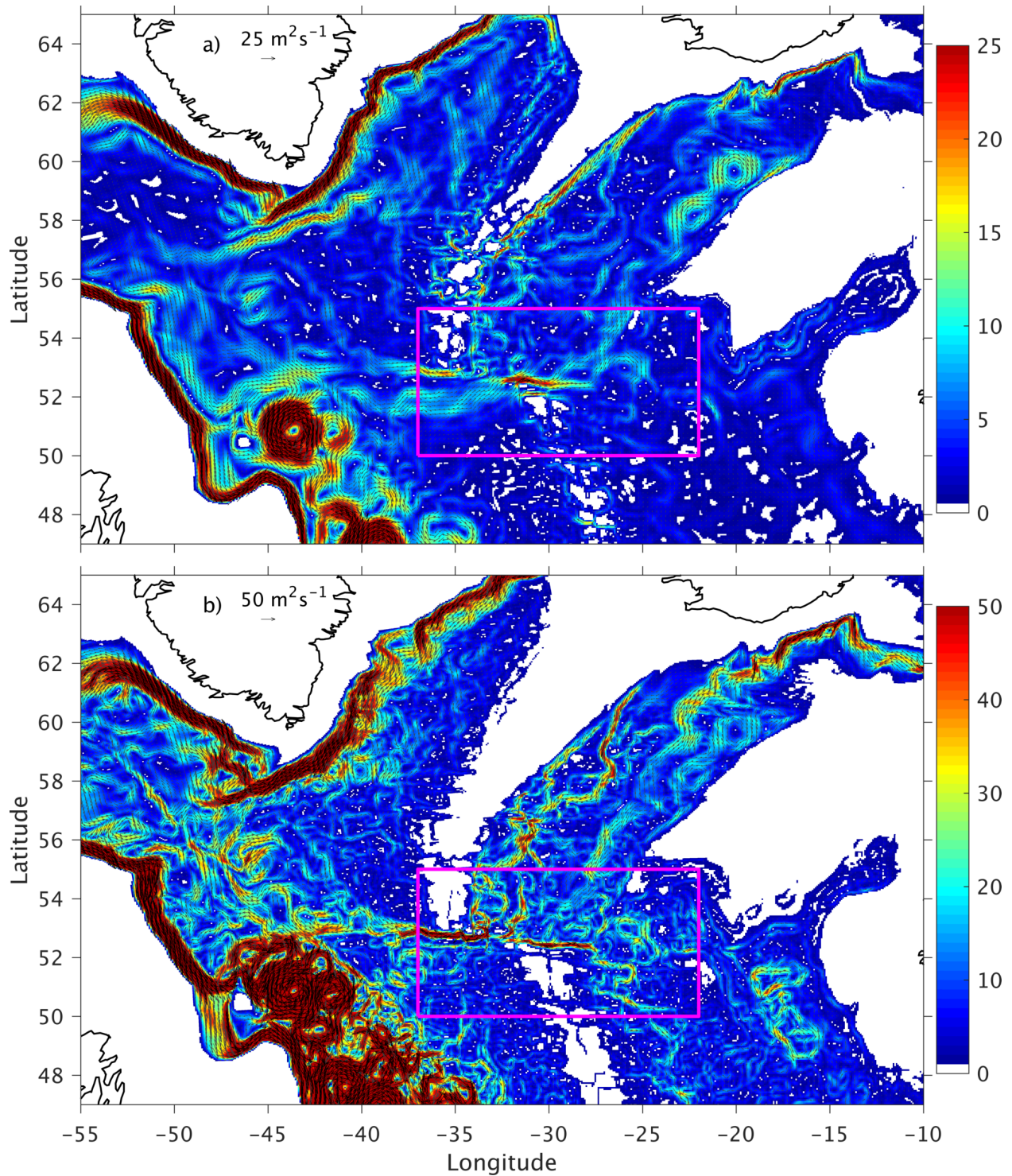
Figure 7. Circulation for the upper and lower parts of the Iceland-Scotland overflow water in the northern North Atlantic. The overflow water flows southward along the western side of the Iceland basin and most of it turns westward to enter the western basins through the Charlie Gibbs Fracture Zone.
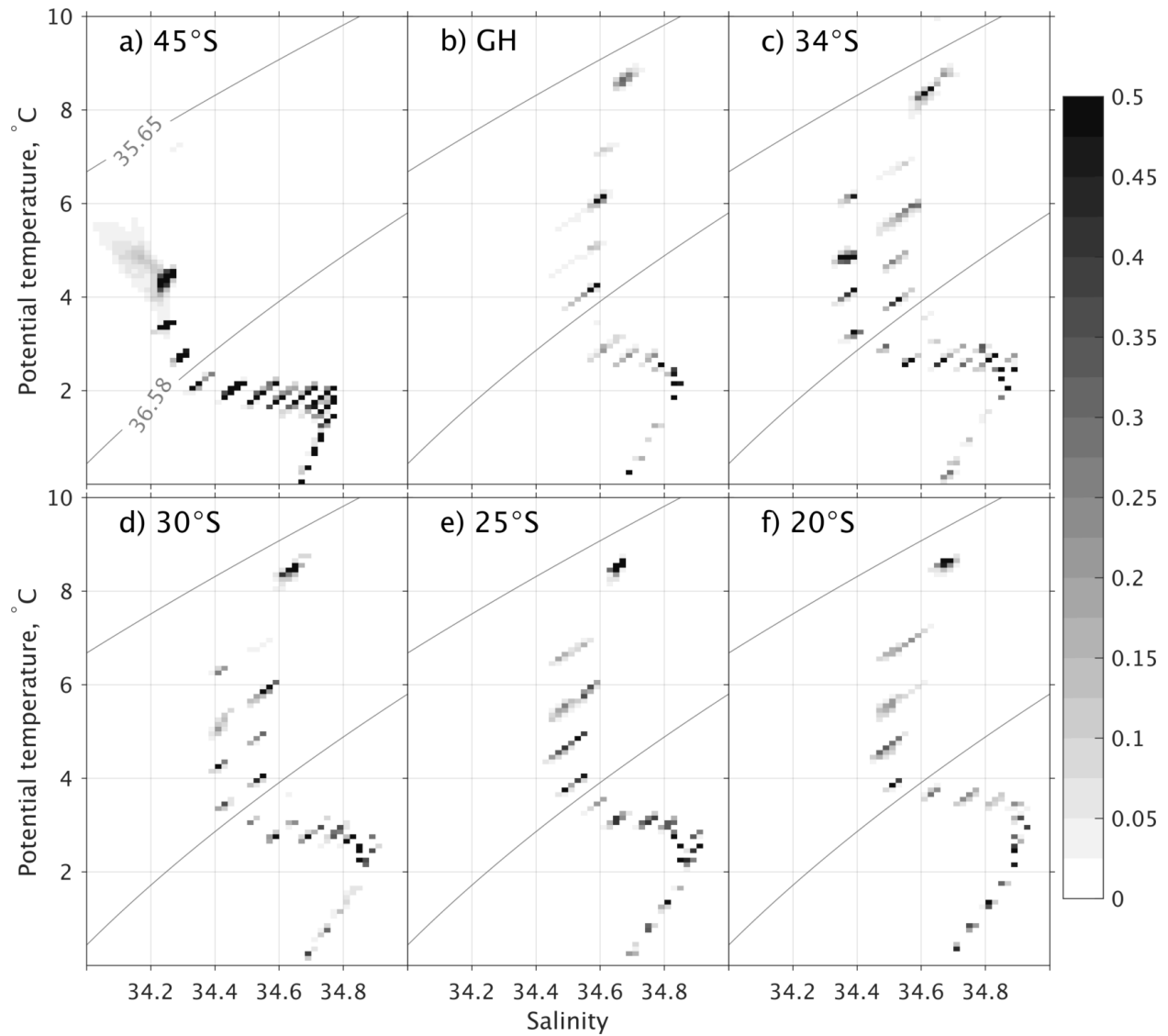
Figure 8. Northward transport projected on temperature-salinity plane from 6 sections: a) 45°S, b) GH section from 45°S toward Good Hope, South Africa, c-f) trans-Atlantic sections at 34°S, 30°S, 25°S, and 20°S. The results show that the northward transport of AAIW (between isopycnals 35.65 and 36.58) has the cold/fresh source from Drake Passage (south of 45°S) and warm/salty source from Agulhas Current east of GH section. The cold source is primarily found within the subtropical gyre and the warm source continues northward as the AMOC component.